Applied Surface Science 636 (2023) 157816

Contents lists available at ScienceDirect

Applied Surface Science

journal homepage: www.elsevier.com/locate/apsusc

Full Length Article

Electric field effect of sliding graphene/hexagonal boron nitride heterobilayer

Bowen Shi [a,b,1], Haotian Wang [a,1], Wen Jiang [a], Yuan Feng [a], Pan Guo [a,*], Heng Gao [a], Zhibin Gao [c,*], Wei Ren [a,*]

[a] Physics Department, Materials Genome Institute, Shanghai Key Laboratory of High Temperature Superconductors, State Key Laboratory of Advanced Special Steel, International Centre of Quantum and Molecular Structures, Shanghai University, Shanghai 200444, China
[b] Shanghai World Foreign Language Academy, 400 Baihua Street, Shanghai 200233 China
[c] State Key Laboratory for Mechanical Behavior of Materials, Xi'an Jiaotong University, Xi'an 710049, China

ARTICLE INFO

Keywords:
Graphene/h-BN heterobilayer
Sliding
Electric dipoles
Electric field

ABSTRACT

The first-principles computer-aided design of atomistic heterostructures can discover the physical properties of new materials and help them widely find applications in frontier scientific fields. Here, we report an investigation on the heterobilayer composed of one sheet of two-dimensional (2D) graphene on the surface of one-layer hexagonal boron nitride (h-BN). We calculate and simulate the binding energies, electric dipoles related to interlayer sliding, and twisting angles of three stacking orders in graphene/hBN heterobilayer. The relative energies of these three heterobilayers are obtained by using first-principles calculations method and the AB stacking structure exhibits the lowest energy. We have also found that the electric field perpendicular to the 2D plane can control the dipole magnitude of the bilayer system, and even change the polarization direction. We studied the kinetic stability of graphene-hBN bilayer heterostructures under the action of external electric fields using *Ab initio* molecular dynamics (AIMD), as well as the thermodynamic stability. Finally, we propose that the graphene/h-BN heterobilayer might play an important role in the field of information electronics as a 2D material with interesting physical properties.

1. Introduction

As a kind of carbon allotrope structure that is made of a single sheet of graphite, graphene has a similar basic unit of many renowned carbon materials at the nanoscale, like Buckminster Fullerene[1], carbon nanotubes and so on. These zero and one-dimensional systems are of great interest as the research topics of future technology, such as computers made of carbon nanotubes[2]. The two-dimensional (2D) honeycomb-like crystal of graphene is composed of regularly extended hexagons with sp^2 orbital hybridization, making the structure extremely stable. The gray-black trace left behind a pencil gently scratching across the paper might have multilayer graphene, while single and double layers of graphene are actually transparent because they are too thin[3]. Experimentally, graphene can be produced in a variety of ways, including chemical vapor deposition, metal catalysis, and mechanical exfoliation[4–6]. The first experimental discovery of graphene was attributed to Geim and Novoselov, who obtained graphene with stable existence in the laboratory by the hand-tearing tape method in 2004[7]. This fantastic discovery had a significant influence on the scientific community in general, and indeed graphene has extremely high smoothness and also many other great functional properties. Specifically, in terms of its mechanical characteristics, graphene has a tensile strength of 125 GPa and an elastic modulus of 1.1 TPa[4,8]. The thermal conductivity of graphene can reach 5500 W/(m K), therefore, graphene composites are widely available for thermal applications with tunable properties[9–11]. For optical property, graphene absorbs only 2.3% of visible light, reflects less than 0.1%, and transmits about 97.7%[12–14]. With an electrical conductivity of 10^6 S/m, graphene is also the best 2D conductor among all known materials at room temperature[15,16]. Many important applications are expected for graphene to be used in electronics and information technology fields. Owing to its excellent electrical conductivity, graphene can be employed in supercapacitors, electrodes, or gadgets which are compatible with silicon electronics. Graphene also holds promise for solar photovoltaic devices, transparent

* Corresponding authors.
E-mail addresses: guopan@shu.edu.cn (P. Guo), zhibin.gao@xjtu.edu.cn (Z. Gao), renwei@shu.edu.cn (W. Ren).
[1] These authors contributed equally.

https://doi.org/10.1016/j.apsusc.2023.157816
Received 17 March 2023; Received in revised form 31 May 2023; Accepted 16 June 2023
Available online 17 June 2023

conductive films, and field effect transistors. Furthermore, the integration of graphene to metals, polymers, and ceramics etc. can dramatically enhance the conductivity and strength of the original materials.

However, a zero bandgap of graphene limits its applications, particularly in nano-electronic semiconductor devices. In recent years, in order to reveal more unique properties, scientists have twisted *bilayer* graphene at precisely controlled angles to make so-called "magic-angle" graphene[17]. Very surprisingly, such a bilayer graphene gives rise to extraordinary correlated electronic effects. In 2018, Cao *et al.* successfully demonstrated that the bilayer graphene twisted by 1.1° presented the unconventional superconductivity at the temperature of 70 mK[17]. Other twisting angles may also be special, like 1.14 or 1.27° where the exotic superconductivity is tunable as verified by others[18]. One may easily see the periodic moiré pattern by twisting bilayer graphene, a common phenomenon when two layers are commensurate as shown in Fig. 1. In fact, attributed to the interference of light, moiré patterns are also popular in optical physics.

In addition, 2D hexagonal boron nitride (h-BN) with similar atomic structure has lattice constants that are very close to graphene, with only 1–2% lattice mismatch[19]. Although 2D h-BN also has graphene-like hexagonal structure, known as "white graphene"[20], the electronic property of h-BN is completely different from graphene. The most significant difference is that h-BN is an electric insulator, though at room temperature the thermal conductivity of h-BN is up to 400 W/(m K) [21]. Optically, h-BN can absorb the ultraviolet band but does not absorb the light of visible wavelength. Gao *et al.* showed that at wavelength of 251 nm, the absorption capacity of h-BN reaches its peak[22]. Since single layer h-BN was successfully prepared by the Manchester group in 2005 by using a micromechanical exfoliation method[23], its excellent insulating properties have been found to be applicable in the bendable capacitors[24,25], as well as in batteries because it accelerates the diffusion of lithium ions[26,27]. The antioxidant properties of h-BN allow it to be used as a protective film for metal substrates[28]. The h-BN can also be applied as a catalyst in the oxidative dehydrogenation of propane[29].

More recently, the combinations of 2D materials have become the new focus of investigation worldwide. For instance, transition metal disulfides MoS_2 and WS_2 heterostructures have been found to be excellent ferroelectric and piezoelectric materials[30]. MoS_2/WSe_2 heterostructure is also a good candidate for photoelectric material[31]. Graphene and h-BN heterostructures [32] are therefore interesting to be studied as presented in this work. Previous theoretical results showed that graphene's optical property in the visual region is not affected by the h-BN substrate [33]. Experiments done by Yang *et al.* also revealed that the h-BN does not influence graphene's photoelectric property[34]. For electronic transport, the mobility of graphene is as high as 10^5 $cm^2V^{-1}s^{-1}$ in graphene/h-BN heterostructure[35,36]. Wang *et al.* reported inversion symmetry breaking induced band gaps of 100 and 160 meV, at the second generation Dirac cones and the original graphene Dirac cone [37]. In brief, the heterogeneous structures of graphene and h-BN might have superior properties and potential applications in many frontier areas.

In this work, we simulate the graphene/h-BN interlayer bilayers and obtained three types of stacking orders of various interlayer sliding. Also, we have calculated the energy versus interlayer distances and found the most stable structure is AB stacking which has the lowest energy. The rotation of the graphene/h-BN heterobilayer and the moiré periodic superstructures are explored. We further revealed the relationship between dipole vector and the external electric field for the three stackings. Finally, we simulated the translational displacement of graphene/h-BN bilayer driven by electric field in the *ab initio* molecular dynamics (AIMD).

2. Method

We use here first-principles calculations based on density functional theory (DFT) and employ the Vienna *ab initio* Simulation Package (VASP) to predict geometric and electrical properties[38]. The electron exchange and correlation functionals were treated by the generalized gradient approximation of Perdew-Burke-Ernzerhof (PBE)[39]. The van der Waals correction D3 was also taken into consideration[40]. The kinetic-energy cutoff of the plane-wave basis was set to 600 eV, and a vacuum space of 25 Å was applied. The Monkhorst-Pack mesh with 12 × 12 × 1 was used for geometry relaxation and single-point energy

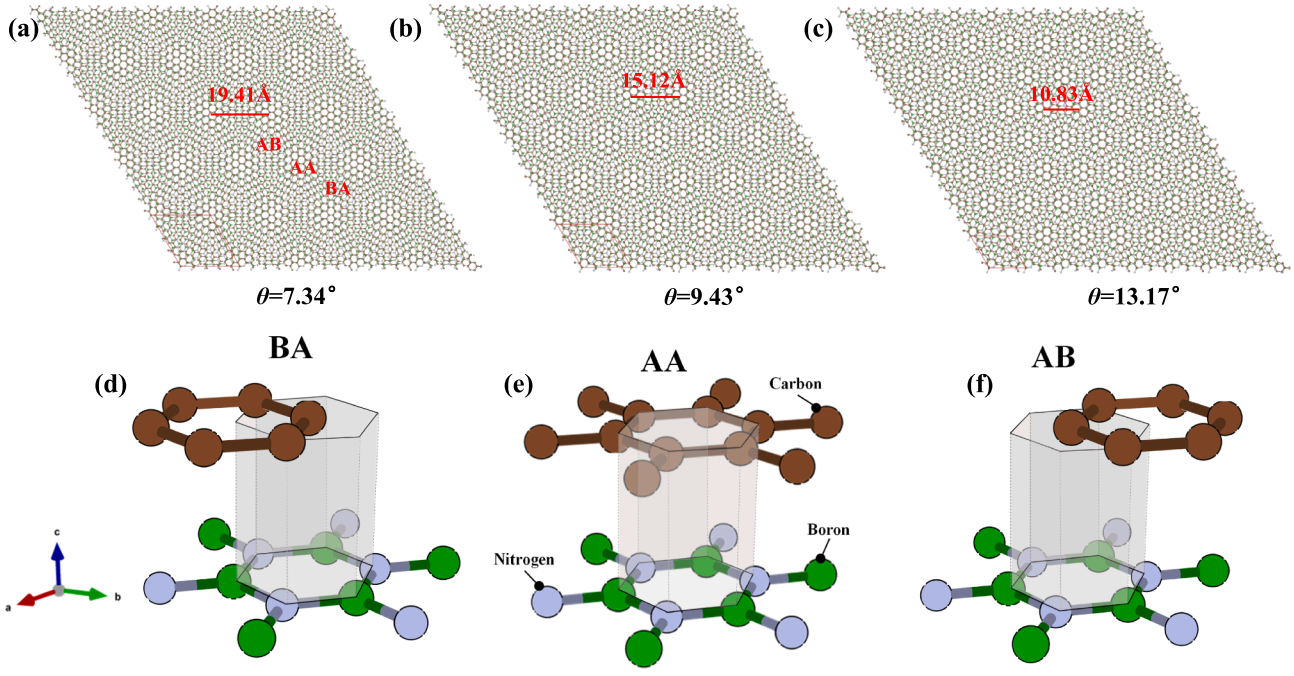

Fig. 1. (a)-(c) Three representative examples of different twisting angles from the AA stacking. The larger the twisting angle is, the smaller the number of atoms is included within the periodic supercells which form the moiré patterns. (d)-(f) Three different stacking orders of graphene/h-BN hetero-bilayers, namely BA, AA, and AB stackings. The brown, green, and gray balls represent carbon, boron, and nitrogen atoms, respectively.

calculations for these optimized geometries. The system used for the AIMD simulation under the NVT ensemble is a supercell of 200 atoms with 100 C atoms, 50 B atoms and 50 N atoms. AIMD is run by first-principles material calculations and simulation of software CP2K. The heat bath method used for the entire temperature control process is Nose-Hoover thermostat. The initial and maintained temperatures were set to 300 K with a time step of 1.0 fs and a total simulation time of 40 ps.

3. Results and discussion

Stacking orders are always an interesting topic in 2D multilayer structure including graphene and 2D h-BN. The bilayer h-BN can be classified into six stacking orders by checking parallel and antiparallel B-N bonds between two layers[41], however, there are two common stacking orders for bilayer graphene. Here, we investigate three types of graphene/h-BN heterobilayer, namely AA, AB and BA stacking orders as shown in Fig. 1. For the AA stacking, two C atoms of the upper graphene layer are located directly above the B and N atoms of the lower h-BN layer. As the AA stacking slides along the C–C bond (bond length of C–C is about 1.44 Å) one may find the AB and BA stackings. In the AB stacking, one C atom overlaps the lower B atom and the other C atom is above the center of the BN hexagon; while in the BA stacking, one C atom overlaps the lower N atom and the other C atom is above the center of the hexagon.

To further investigate the relevant physical properties of the three stacking orders, structural optimization is carried out by means of DFT to obtain a more reasonably relaxed structure. After structural optimization, the in-plane lattice constants of the three stackings are almost the same, about 2.49 Å. Very interestingly, the interlayer spacing of three stackings are found to be quite different. The interlayer spacings of AA, AB and BA stackings are 3.54 Å, 3.33 Å and 3.50 Å, respectively, which are so-called equilibrium distances. The reason for this phenomenon is related to the attraction of electrons in graphene with cation B atoms and the repulsion of electrons in graphene with anion N atoms. It is worth mentioning that whether it is bilayer graphene, bilayer boron nitride, or graphene/boron nitride heterobilayer, the force between the layers is of van der Waals type, which is much weaker than chemical bonding. For the AB stacking, where the C atom has the lowest charge density and thus the graphene layer has a stronger attractive interaction with the BN layer and thus the smallest interlayer distance.

Since the striking discovery of "magic-angle" graphene by Cao *et al.*, twisting electronics also called twistronics has caused a new focus of research in the physics community worldwide[17]. We have tried to construct the twisted graphene/h-BN heterobilayer from graphene and 2D h-BN[42–44]. We chose the rotation axis as the vertical line where the C atom located above the B atom of the BN layer in AA stacking. Fig. 1(a)-(c) show the schematic diagrams of the structures we obtained by rotating 7.34°, 9.43°, and 13.17° around the rotation axis, respectively. The structures are consistent with the results in Supplemental Material Table S1, which have 244, 148, and 76 atoms respectively. It is clear that when the rotation angle is smaller, the supercell formed is larger and the number of atoms is greater. Therefore, for small twisting angles the superlattice structure requires longer periodic distances to repeat the same translational unit cells. Table S1 of the Supplementary Material gives the theoretical results for the twist angles and the associated number of primitive units. There are four atoms in each primitive unit (two carbons, one nitrogen, and one boron), so the total number of atoms is four times the number of primitive units.

In addition to torsion, sliding can also be achieved to change the stacking order of the graphene/h-BN heterobilayer. Various different sliding paths are discussed here, among which two paths along the diagonal of the hexagonal lattice allow the polarization direction to be inverted, as shown in Figs. 2 and 3. The directions of these two paths are (-1,1,0) and (1,-1,0), respectively. In the path I (-1,1,0), the slip distance is about 1.44 Å, while in the path II (1,-1,0), the slide process results in an AA stacking order with a sliding distance of about 2.88 Å. The polarization in the graphene/h-BN heterobilayer is generated by the electric dipole moments, while the electric dipole is caused by the non-coincidence of the centers of positive and negative charges in the structure. The polarization directions of the AB and BA stackings are

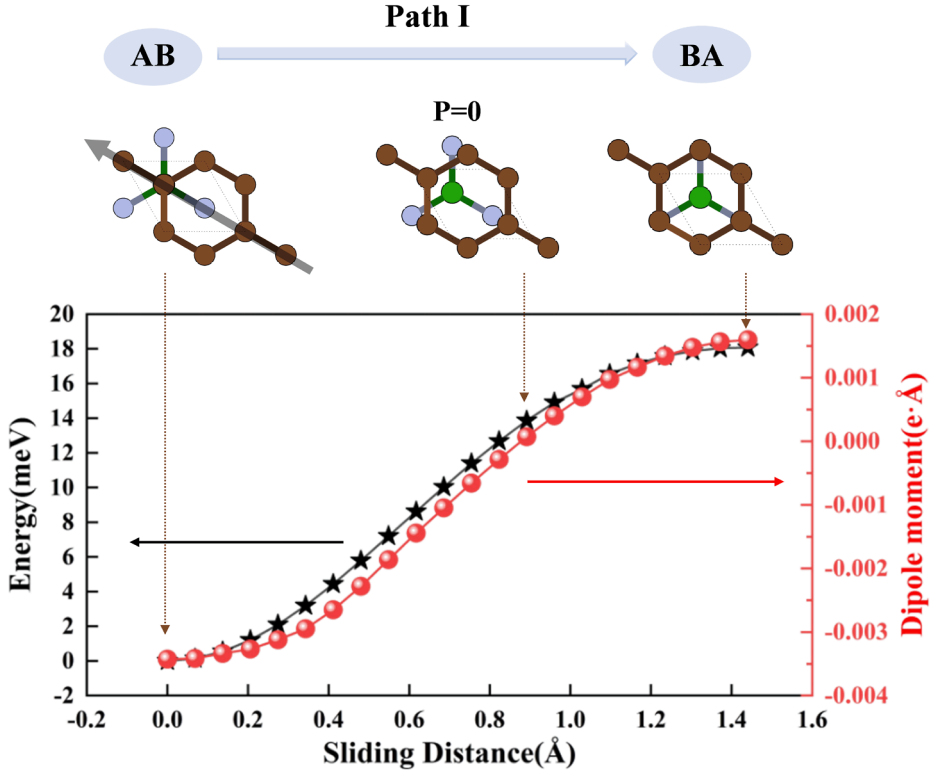

Fig. 2. The energy and dipole moment versus sliding distance along the path I, from AB to BA stacking.

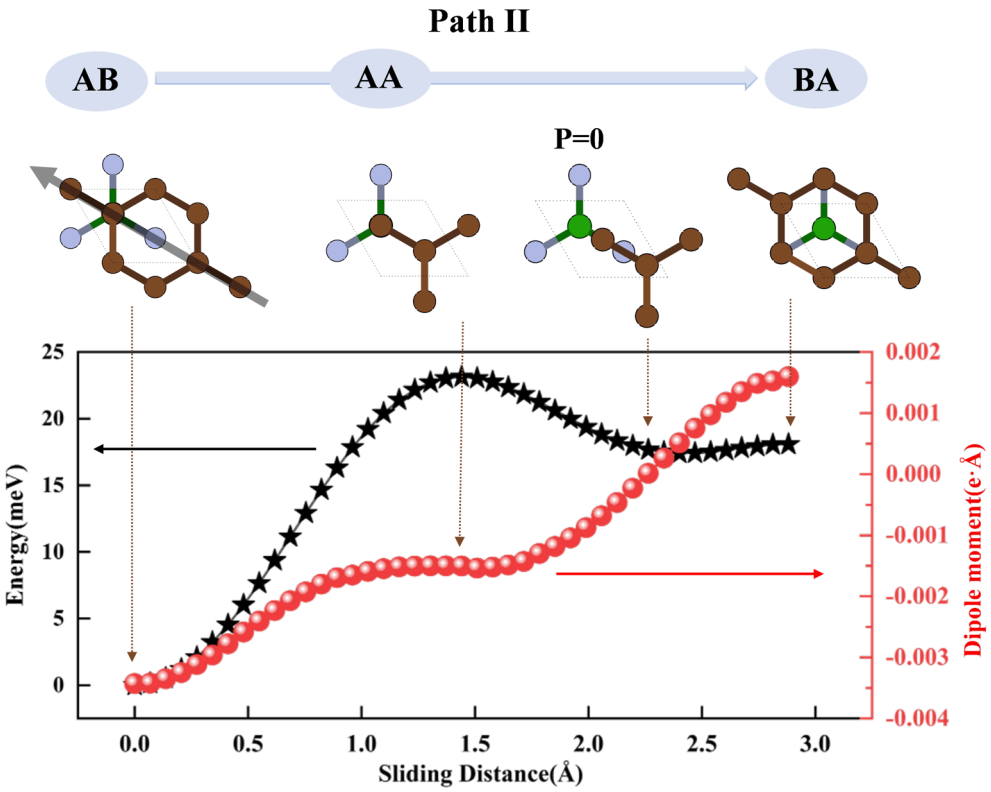

Fig. 3. The energy and dipole moment versus sliding distance along the path II, from AB to BA while through AA stacking.

reversed, but the polarization values are not equal in magnitude as ferroelectrics. In both sliding paths, the dipole moment values are slowly changing, and the polarization values are indeed related to the change of stacking order. We found that in both paths there are two stacking structures in which the dipole values are 0 because they have no charge transfer between the layers, suggesting that the sliding can change the polarization reversal.

We know that the binding energy can be used to evaluate the energetic stability of a heterostructure. Usually, the binding energy is defined by the following equation:

$E_b = E(AB) - E(A) - E(B)$.

For graphene/h-BN heterobilayer, we have:

$E(AB) = E(\text{graphene/h-BN})$, $E(A) = E(\text{graphene})$, $E(B) = E(\text{h-BN})$.

The Supplemental Material Table S2 displays the variation of the binding energy with the layer spacing for our three calculated stackings. From the table, we see that the binding energy (absolute value) of AB stacking is the lowest for the three stackings at their respective equilibrium spacing, so the AB stacking is the most stable. This is consistent with our results shown in Fig. 4 and it can be seen that the energy decreases dramatically when the layer spacing decreases and then increases sharply when bilayer getting too close to each other, which shows that the graphene/h-BN heterobilayer is very sensitive to change of interlayer distances.

When a classical or quantum state of matter is at the lowest energy level, we usually say that it is the ground state. The DFT approach in our present work is capable to deal with the ground state for which we did not consider higher energy level, or excited state, by electrons absorbing energy. Because the systems generally tend to occupy the state with the lowest energy, the ground state is an important aspect of studying bilayers here. Therefore, we calculated the ground state energies of the three mentioned stackings. The AB stacking is found to have the lowest energy, while the AA stacking having 17 meV higher energy, and the BA

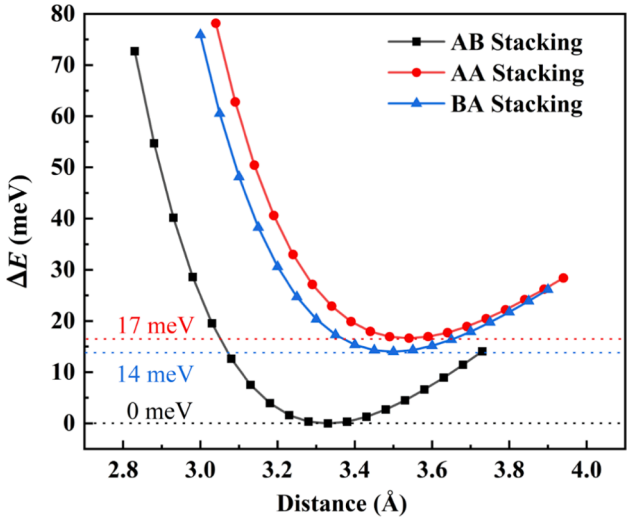

Fig. 4. The relationship between the relative energy and the graphene/h-BN interlayer distance. We set the zero-energy point as the minimal energy of AB stacking at 3.33 Å.

stacking having 14 meV higher energy than the AB stacking. Hence, among the three structures, the AB should be the most stable, the AA is the least stable, and the BA is somewhat in between. Many 2D materials are highly susceptible to stimulation by the external environment, so we investigated the effect of applying vertical pressure on the energy of the bilayers. In brief, we compared the energy of structures with different interlayer distance. We thus compressed and stretched each of the three stackings in the vertical direction to decrease and increase the bilayer spacing between graphene and h-BN. We found that regardless of the type of stackings, the more their layer spacing deviated from the equilibrium spacing, the higher the energy, suggesting that the structure

became more unstable. However, when the bilayer spacing is large enough, their energies basically converge. This is rather reasonable that when the interlayer distance is too far for atomistic interaction to make an influence. Our obtained results agree very well with previously reported studies[19,45].

For the AB stacking, the graphene/h-BN bilayer polarization (total dipole per unit area) is found to be 0.960 pC/m, which is oriented along the *c*-axis, or vertically upward; for the AA stacking, its polarization is 0.333 pC/m, which is oriented in the same direction as AB, also vertically upward; whereas for the BA stacking, its polarization is 0.216 pC/m, but in the opposite direction in contrast with the AB and AA stackings. Based on that, we applied electric fields up to 0.05 V/ Å in magnitude to these three stackings, as shown in Fig. 5. We found that with the gradual increase of electric field strength, the polarization direction of AB stacking flipped direction at the electric field strength of 0.025 V/Å, while the polarization switching of BA and AA stackings occur at 0.005 V/Å and 0.01 V/Å, respectively.

To further understand the possible in-plane movement process between graphene/h-BN heterobilayer, we perform the AIMD simulations under the external electric field to investigate the microscopic mechanism. We have observed the field induced interlayer sliding during the simulations in Supplemental Material Fig. S1, and we plotted the temperature and energy variation versus time results obtained from the molecular dynamics simulations in Supplemental Material Fig. S2. The

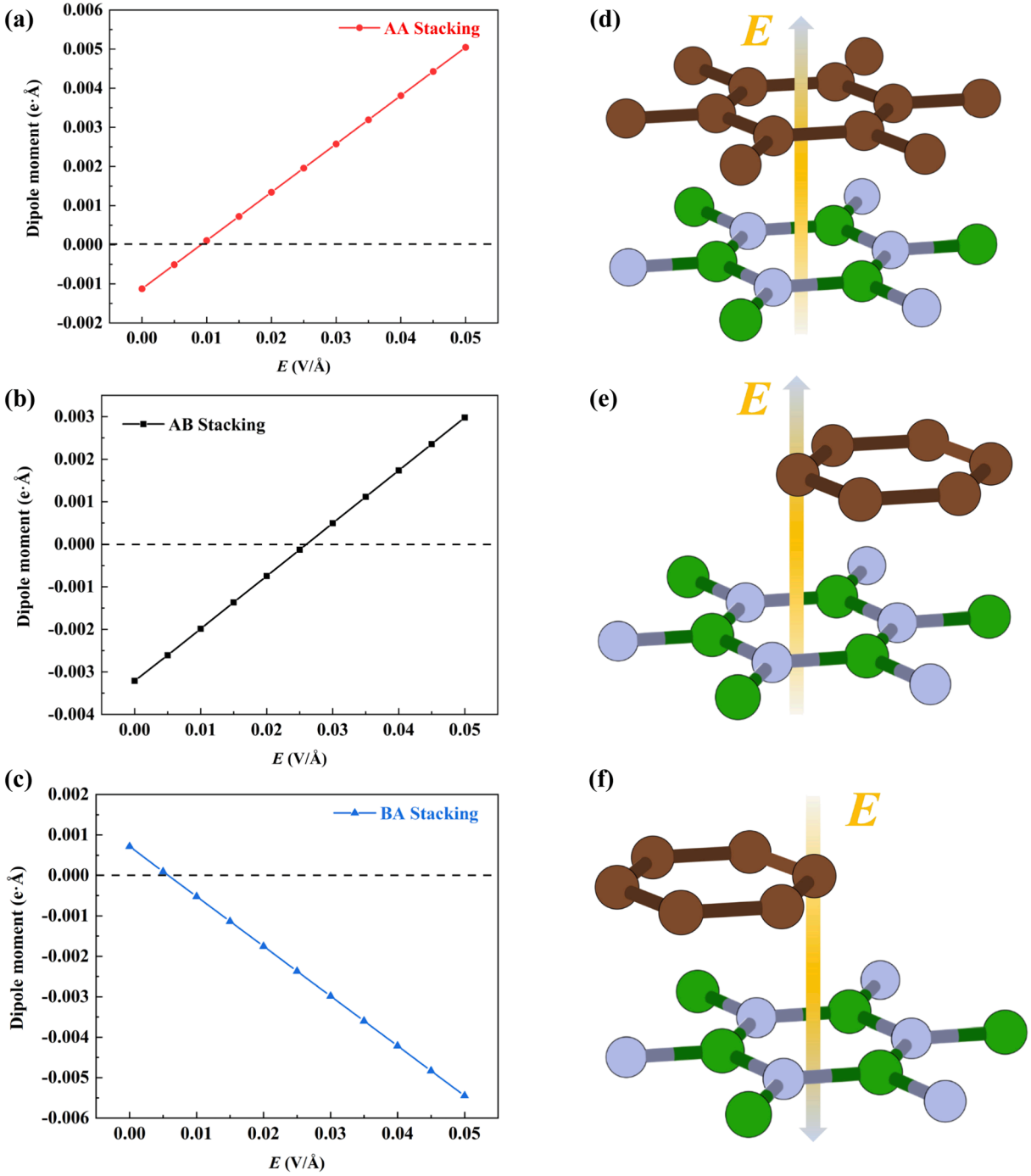

Fig. 5. (a)-(c) show the relationships between dipole moments and externally applied electric field, with the polarization direction switching at the crossing points on the dashed lines. (d)-(f) illustrate the stacking orders of each P-E curve, and also show the direction of the applied electric fields.

visualization of the simulated process snapshots of molecular dynamics is shown in Supplemental Material Fig. S1. Initially, the bilayer structure is an AA stacking, and the stacking order of the structure changes rapidly under the external applied electric field of 2 V/Å. After about 975 fs, the system transforms to be close to the AB stacking. At about 1475 fs, the system shows BA stacking and continues to move. At about 1844 fs, the system returns to AB stacking and thereafter, the structure stays at AB stacking. This simulation process is also consistent with the previous conclusion that the energy of AB stacking is the lowest. When a sufficiently large external electric field is applied, the direction of the dipole moment is reversed and the spontaneous polarization direction of the whole system changes at the same time. As shown in Fig. S2(a), the temperature is maintained almost around 300 K with very little fluctuation after the system reaches equilibrium. This also reflects that the whole simulation process is quite reasonable. The energy versus time for the whole simulation process is shown in Fig. S2(b). The corresponding fluctuations of the total energy oscillate in a very narrow range under the influence of temperature, indicating that this state should be thermally stable. Additionally, we have investigated the influence of temperature on the stability of the graphene/h-BN heterobilayer under an external electric field. Fig. S3 depicts the energy fluctuations of the graphene/h-BN heterobilayer at a temperature of 400 K and an applied electric field of 0.05 eV/Å. Throughtout the simulation, we observe that the geometric shape of the heterobilayer remains unchanged, without bond breakage or phase transition, indicating the excellent stability of the graphene/h-BN heterobilayer.

The graphene/h-BN heterobilayer has a wide range of potential applications in the field of emerging electronics. It can be utilized for the fabrication of field-effect transistors[35,46,47], leveraging graphene's high carrier mobility and h-BN's wide bandgap to enhance device performance and speed. In addition, graphene/h-BN/GaAs sandwich diode has been demonstrated to make solar cells with higher power conversion efficiency and photodetectors with increased on/off ratio[48]. Furthermore, this heterostructure exhibits promising potential in other areas, such as thermoelectric devices[49], light-emitting diodes[50], pressure sensors[51], and nanocapacitors[52]. These examples exemplify the advantages of the graphene/h-BN heterobilayer in nanoscale functional components, presenting significant potential and practical significance. However, implementing these unique materials in experiment requires further research and development to overcome many challenges and limitations for achieving high-quality heterostructures, optimizing interface quality, developing scalable fabrication processes, and integration technologies. Importantly, ensuring stability, reliability, and long-term device performance are critical factors to consider in reality. In the long term, such heterostructure materials are expected to play an increasingly significant role in the information age, offering expanded possibilities for future devices and systems.

4. Conclusions

We explored the physical properties of the graphene/h-BN heterobilayer to discuss the interlayer stacking, twisting and sliding phenomena. We constructed the graphene/h-BN heterobilayers with three configurations of AA, AB and BA stackings. Then we obtained the graphene/h-BN heterobilayer upon twisting the interlayer angles, and found the periodic superstructures of moiré patterns. We calculated from first principles the variation of energy with respect to the layer spacing for the three stacking orders. Interestingly, we checked the existence of out-of-plane polarization in the three stackings, and studied the relationship between the dipole moment strength and the applied electric field which could even change the polarization direction. Finally, we investigated the microscopic mechanism by simulating the interlayer motion and physical property changes of the heterobilayer under the external electric field. Our molecular dynamics results are in excellent agreement with the density functional theory energy values, further verifying that the ground state structure of graphene/h-BN is the AB stacking.

CRediT authorship contribution statement

Bowen Shi: Writing – original draft, Methodology, Data curation, Investigation, Visualization. **Haotian Wang:** Data curation, Methodology, Investigation, Visualization. **Wen Jiang:** Investigation, Visualization, Software. **Yuan Feng:** Investigation, Methodology. **Pan Guo:** Writing review & editing, Funding acquisition. **Heng Gao:** Writing review & editing, Methodology. **Zhibin Gao:** Writing review & editing, Funding acquisition. **Wei Ren:** Writing review & editing, Resources, Supervision, Funding acquisition, Project administration.

Declaration of Competing Interest

The authors declare that they have no known competing financial interests or personal relationships that could have appeared to influence the work reported in this paper.

Data availability

No data was used for the research described in the article.

Acknowledgments

This work was supported by National Natural Science Foundation of China (12074241, 11929401, 52120204, 12104287, 12104356 and 52250191), Science and Technology Commission of Shanghai Municipality (22XD1400900, 20501130600, 21JC1402700, 21JC1402600, 22YF1413300), High-Performance Computing Center, Shanghai Technical Service Center of Science and Engineering Computing, Shanghai University.

Appendix A. Supplementary data

Supplementary data to this article can be found online at https://doi.org/10.1016/j.apsusc.2023.157816.

References

[1] H.W. Kroto, J.R. Heath, S.C. O'Brien, R.F. Curl, R.E. Smalley, C60: Buckminsterfullerene, Nature 318 (1985) 162.
[2] M.M. Shulaker, G. Hills, N. Patil, H. Wei, H.-Y. Chen, H.-S.-P. Wong, S. Mitra, Carbon nanotube computer, Nature 501 (2013) 526.
[3] Y. Tang, C.S. Lee, Z. Chen, G. Yuan, Z. Kang, L. Luo, H. Song, Y. Liu, Z. He, W. Zhang, High-quality graphenes via a facile quenching method for field-effect transistors, Nano Lett. 9 (2009) 1374.
[4] K.S. Kim, Y. Zhao, H. Jang, S.Y. Lee, J.M. Kim, K.S. Kim, J.-H. Ahn, P. Kim, J.-Y. Choi, B.H. Hong, Large-scale pattern growth of graphene films for stretchable transparent electrodes, Nature 457 (2009) 706.
[5] P.W. Sutter, J.-I. Flege, E.A. Sutter, Epitaxial graphene on ruthenium, Nat. Mater. 7 (2008) 406.
[6] C. Berger, Z. Song, X. Li, X. Wu, N. Brown, C. Naud, D. Mayou, T. Li, J. Hass, A. N. Marchenkov, Electronic confinement and coherence in patterned epitaxial graphene, Science 312 (2006) 1191.
[7] K.S. Novoselov, A.K. Geim, S.V. Morozov, D.-E. Jiang, Y. Zhang, S.V. Dubonos, I. V. Grigorieva, A.A. Firsov, Electric field effect in atomically thin carbon films, Science 306 (2004) 666.
[8] K.I. Bolotin, K.J. Sikes, Z. Jiang, M. Klima, G. Fudenberg, J. Hone, P. Kim, H. L. Stormer, Ultrahigh electron mobility in suspended graphene, Solid State Commun. 146 (2008) 351.
[9] A.A. Balandin, Thermal properties of graphene and nanostructured carbon materials, Nat. Mater. 10 (2011) 569.
[10] L. Falkovsky, Symmetry constraints on phonon dispersion in graphene, Phys. Lett. A 372 (2008) 5189–5192.
[11] E. Pop, V. Varshney, A.K. Roy, Thermal properties of graphene: Fundamentals and applications, MRS Bull. 37 (2012) 1273.
[12] A.B. Kuzmenko, E. Van Heumen, F. Carbone, D. Van Der Marel, Universal optical conductance of graphite, Phys. Rev. Lett. 100 (2008), 117401.
[13] J.-P. Salvetat, J.-M. Bonard, R. Bacsa, T. Stöckli, L. Forró, Physical properties of carbon nanotubes, in: AIP Conference Proceedings, 1998, pp. 467.
[14] L.A. Falkovsky, Optical properties of graphene, in: Journal of Physics: Conference Series, IOP Publishing, 2008, p. 012004.
[15] A.C. Neto, F. Guinea, N.M. Peres, K.S. Novoselov, A.K. Geim, The electronic properties of graphene, Rev. Mod. Phys. 81 (2009) 109.

[16] K. Novoselov, S. Morozov, T. Mohinddin, L. Ponomarenko, D. Elias, R. Yang, I. Barbolina, P. Blake, T. Booth, D. Jiang, Electronic properties of graphene, Physica Status Solidi (b) 244 (2007) 4106.
[17] Y. Cao, V. Fatemi, S. Fang, K. Watanabe, T. Taniguchi, E. Kaxiras, P. Jarillo-Herrero, Unconventional superconductivity in magic-angle graphene superlattices, Nature 556 (2018) 43.
[18] M. Yankowitz, S. Chen, H. Polshyn, Y. Zhang, K. Watanabe, T. Taniguchi, D. Graf, A.F. Young, C.R. Dean, Tuning superconductivity in twisted bilayer graphene, Science 363 (2019) 1059.
[19] G. Giovannetti, P.A. Khomyakov, G. Brocks, P.J. Kelly, J. Van Den Brink, Substrate-induced band gap in graphene on hexagonal boron nitride: Ab initio density functional calculations, Phys. Rev. B 76 (2007), 073103.
[20] L. Song, L. Ci, H. Lu, P.B. Sorokin, C. Jin, J. Ni, A.G. Kvashnin, D.G. Kvashnin, J. Lou, B.I. Yakobson, Large scale growth and characterization of atomic hexagonal boron nitride layers, Nano Lett. 10 (2010) 3209.
[21] C. Zhi, Y. Bando, C. Tang, H. Kuwahara, D. Golberg, Large-scale fabrication of boron nitride nanosheets and their utilization in polymeric composites with improved thermal and mechanical properties, Adv. Mater. 21 (2009) 2889.
[22] R. Gao, L. Yin, C. Wang, Y. Qi, N. Lun, L. Zhang, Y.-X. Liu, L. Kang, X. Wang, High-yield synthesis of boron nitride nanosheets with strong ultraviolet cathodoluminescence emission, J. Phys. Chem. C 113 (2009) 15160.
[23] K.S. Novoselov, D. Jiang, F. Schedin, T. Booth, V. Khotkevich, S. Morozov, A.K. Geim, Two-dimensional atomic crystals, Proc. Natl. Acad. Sci., 102 (2005) 10451-10453.
[24] N. Guo, J. Wei, Y. Jia, H. Sun, Y. Wang, K. Zhao, X. Shi, L. Zhang, X. Li, A. Cao, Fabrication of large area hexagonal boron nitride thin films for bendable capacitors, Nano Res. 6 (2013) 602.
[25] C.K. Maity, G. Hatui, S. Sahoo, P. Saren, G.C. Nayak, Boron nitride based ternary nanocomposites with different carbonaceous materials decorated by polyaniline for supercapacitor application, ChemistrySelect 4 (2019) 3672.
[26] Y. Yi, H. Li, H. Chang, P. Yang, X. Tian, P. Liu, L. Qu, M. Li, B. Yang, H. Li, Few-layer boron nitride with engineered nitrogen vacancies for promoting conversion of polysulfide as a cathode matrix for lithium-sulfur batteries, Chem.–A Eur. J. 25 (2019) 8112.
[27] Y. Mussa, F. Ahmed, M. Arsalan, E. Alsharaeh, Two dimensional (2D) reduced graphene oxide (RGO)/hexagonal boron nitride (h-BN) based nanocomposites as anodes for high temperature rechargeable lithium-ion batteries, Sci. Rep. 10 (2020) 1.
[28] L.H. Li, Y. Chen, Atomically thin boron nitride: unique properties and applications, Adv. Funct. Mater. 26 (2016) 2594.
[29] J. Grant, C.A. Carrero, F. Goeltl, J. Venegas, P. Mueller, S.P. Burt, S. Specht, W. McDermott, A. Chieregato, I. Hermans, Selective oxidative dehydrogenation of propane to propene using boron nitride catalysts, Science 354 (2016) 1570.
[30] L. Rogée, L. Wang, Y. Zhang, S. Cai, P. Wang, M. Chhowalla, W. Ji, S.P. Lau, Ferroelectricity in untwisted heterobilayers of transition metal dichalcogenides, Science 376 (2022) 973.
[31] R. Cheng, D. Li, H. Zhou, C. Wang, A. Yin, S. Jiang, Y. Liu, Y. Chen, Y. Huang, X. Duan, Electroluminescence and photocurrent generation from atomically sharp WSe2/MoS2 heterojunction p–n diodes, Nano Lett. 14 (2014) 5590.
[32] B. Luo, R. Gao, Y. Wang, H. Gao, J. Liu, W. Ren, Stacking Order, Perfect Spin Polarization, and Giant Magnetoresistance in Zigzag $\mathrm{Graphene}/$h-BN Heterobilayer Nanoribbons, Phys. Rev. Appl 19 (2023), 034002.
[33] J. Wang, S. Cao, P. Sun, Y. Ding, Y. Li, F. Ma, Optical advantages of graphene on the boron nitride in visible and SW-NIR regions, RSC Adv. 6 (2016), 111345.
[34] X. Yang, F. Zhai, H. Hu, D. Hu, R. Liu, S. Zhang, M. Sun, Z. Sun, J. Chen, Q. Dai, Far-field spectroscopy and near-field optical imaging of coupled Plasmon–phonon polaritons in 2D van der Waals heterostructures, Adv. Mater. 28 (2016) 2931.
[35] C.R. Dean, A.F. Young, I. Meric, C. Lee, L. Wang, S. Sorgenfrei, K. Watanabe, T. Taniguchi, P. Kim, K.L. Shepard, Boron nitride substrates for high-quality graphene electronics, Nat. Nanotechnol. 5 (2010) 722.
[36] A.S. Mayorov, R.V. Gorbachev, S.V. Morozov, L. Britnell, R. Jalil, L. A. Ponomarenko, P. Blake, K.S. Novoselov, K. Watanabe, T. Taniguchi, Micrometer-scale ballistic transport in encapsulated graphene at room temperature, Nano Lett. 11 (2011) 2396.
[37] E. Wang, X. Lu, S. Ding, W. Yao, M. Yan, G. Wan, K. Deng, S. Wang, G. Chen, L. Ma, Gaps induced by inversion symmetry breaking and second-generation Dirac cones in graphene/hexagonal boron nitride, Nat. Phys. 12 (2016) 1111.
[38] G. Kresse, J. Furthmüller, Efficient iterative schemes for ab initio total-energy calculations using a plane-wave basis set, Phys. Rev. B 54 (1996) 11169.
[39] J.P. Perdew, K. Burke, M. Ernzerhof, Generalized gradient approximation made simple, Phys. Rev. Lett. 77 (1996) 3865.
[40] S. Grimme, J. Antony, S. Ehrlich, H. Krieg, A consistent and accurate ab initio parametrization of density functional dispersion correction (DFT-D) for the 94 elements H-Pu, J. Chem. Phys. 132 (2010), 154104.
[41] W. Jiang, C. Liu, X. Ma, X. Yu, S. Hu, X. Li, L.A. Burton, Y. Liu, Y. Chen, P. Guo, Anomalous ferroelectricity and double-negative effects in bilayer hexagonal boron nitride, Phys. Rev. B 106 (2022), 054104.
[42] M.H. Naik, M. Jain, Ultraflatbands and shear solitons in moiré patterns of twisted bilayer transition metal dichalcogenides, Phys. Rev. Lett. 121 (2018), 266401.
[43] S. Naik, M.H. Naik, I. Maity, M. Jain, Twister: Construction and structural relaxation of commensurate moiré superlattices, Comput. Phys. Commun. 271 (2022), 108184.
[44] M.H. Naik, I. Maity, P.K. Maiti, M. Jain, Kolmogorov-Crespi potential for multilayer transition-metal dichalcogenides: capturing structural transformations in moiré superlattices, J. Phys. Chem. C 123 (2019) 9770.
[45] Y. Fan, M. Zhao, Z. Wang, X. Zhang, H. Zhang, Tunable electronic structures of graphene/boron nitride heterobilayers, Appl. Phys. Lett. 98 (2011), 083103.
[46] K.H. Lee, H.J. Shin, J. Lee, I.Y. Lee, G.H. Kim, J.Y. Choi, S.W. Kim, Large-scale synthesis of high-quality hexagonal boron nitride nanosheets for large-area graphene electronics, Nano Lett 12 (2012) 714–718.
[47] J. Lee, T.J. Ha, K.N. Parrish, S.F. Chowdhury, L. Tao, A. Dodabalapur, D. Akinwande, High-Performance Current Saturating Graphene Field-Effect Transistor With Hexagonal Boron Nitride Dielectric on Flexible Polymeric Substrates, IEEE Electron Device Lett. 34 (2013) 172–174.
[48] X. Li, S. Lin, X. Lin, Z. Xu, P. Wang, S. Zhang, H. Zhong, W. Xu, Z. Wu, W. Fang, Graphene/h-BN/GaAs sandwich diode as solar cell and photodetector, Opt Express 24 (2016) 134–145.
[49] C.-C. Chen, Z. Li, L. Shi, S.B. Cronin, Thermoelectric transport across graphene/hexagonal boron nitride/graphene heterostructures, Nano Res. 8 (2015) 666–672.
[50] F. Withers, O. Del Pozo-Zamudio, S. Schwarz, S. Dufferwiel, P.M. Walker, T. Godde, A.P. Rooney, A. Gholinia, C.R. Woods, P. Blake, S.J. Haigh, K. Watanabe, T. Taniguchi, I.L. Aleiner, A.K. Geim, V.I. Fal'ko, A.I. Tartakovskii, K.S. Novoselov, WSe_2 light-emitting tunneling transistors with enhanced brightness at room temperature, Nano Lett 15 (2015) 8223–8228.
[51] Y. Xu, Z. Guo, H. Chen, Y. Yuan, J. Lou, X. Lin, H. Gao, H. Chen, B. Yu, In-plane and tunneling pressure sensors based on graphene/hexagonal boron nitride heterostructures, Appl. Phys. Lett. 99 (2011), 133109.
[52] G. Shi, Y. Hanlumyuang, Z. Liu, Y. Gong, W. Gao, B. Li, J. Kono, J. Lou, R. Vajtai, P. Sharma, P.M. Ajayan, Boron nitride-graphene nanocapacitor and the origins of anomalous size-dependent increase of capacitance, Nano Lett 14 (2014) 1739–1744.